Majorana fermions at the edge of superconducting islands

R. S. Akzyanov, A. L. Rakhmanov, A. V. Rozhkov, and Franco Nori

Phys. Rev. B **92**, 075432 — Published 21 August 2015

DOI: 10.1103/PhysRevB.92.075432

Majorana fermions at the edge of superconducting islands

R.S. Akzyanov,[1,2,3] A.L. Rakhmanov,[1,2,3,4] A.V. Rozhkov,[1,2,4] and Franco Nori[4,5]

[1]*Moscow Institute of Physics and Technology, Dolgoprudny, Moscow Region, 141700 Russia*
[2]*Institute for Theoretical and Applied Electrodynamics, Russian Academy of Sciences, Moscow, 125412 Russia*
[3]*All-Russia Research Institute of Automatics, Moscow, 127055 Russia*
[4]*CEMS, RIKEN, Saitama, 351-0198, Japan*
[5]*Department of Physics, University of Michigan, Ann Arbor, MI 48109-1040, USA*

(Dated: July 31, 2015)

We investigate the properties of electron states localized at the edge of a superconducting island placed on the surface of a topological insulator in a magnetic field. In such systems, Majorana fermions emerge if an odd number of vortices (or odd multivortex vorticity) is hosted by the island; otherwise, no Majorana states exist. Majorana states emerge in pairs: one state is localized near the vortex core, and another at the island edge. We analyze in detail the robustness of Majorana fermions at the edge of the island threaded by a single vortex. If the system parameters are optimized, the energy gap between the Majorana fermion and the first excited state at the edge is of the order of the superconducting gap induced on the surface of the topological insulator. The stability of the Majorana fermion state against a variation of the gate voltage and its sensitivity to the magnetic field allows one to experimentally distinguish the edge Majorana fermion from conventional Dirac fermions.

PACS numbers: 71.10.Pm, 03.67.Lx, 74.45.+c

I. INTRODUCTION

The possible realization of Majorana fermion states in condensed matter physics is attracting considerable interest in recent years[1–8]. This is partly due to the non-abelian anyonic statistics of Majorana fermions, allowing the realization of topologically-protected quantum gates[9]. Topological quantum computation requires the braiding of anyons[10]. Majorana braiding might be realized by the controllable manipulation of the pairwise interaction between separate Majorana fermions[11–13]. The decoherence caused by the tunneling between Majorana fermions sets an upper limit of the time on the elementary operation, while the energy of the excited states determines the lower time limit of the elementary operation[14]. Many attempts have been performed to find Majorana fermions in different systems. Recently, possible observations of Majorana fermions in quantum nanowires[15,16] and atom chains[17] were reported.

The interface between a topological insulator and an s-wave superconductor (SC) is a promising system for the possible realization of Majorana fermions.[18–22] Such proximity-induced superconductivity is a mixture of s and p-wave correlations.[18,23] Being topologically equivalent to the p-wave superconductivity, it supports Majorana fermions.[24] However, specific features of this superconducting state, in particular, quasiparticle linear dispersion on the surface of the topological insulator, are of importance for the structure and robustness of the Majorana state and requires adequate analysis. Majorana fermions may emerge at the vortex core in the proximity-induced superconducting region on the surface of the topological insulator. However, the minigap separating the Majorana fermion and the Caroli-de Gennes-Matricon (CdGM) levels in the Abrikosov vortex core[25,26] is very small (about 10^{-3} K). In order to increase the robustness of the Majorana state, Ref. 21 proposed to make a hole in the superconducting layer to pin the vortex and to remove the CdGM levels. These ideas were further elaborated in Ref. 27.

Majorana fermions could also localize near boundaries of the superconducting region. However, such states have attracted much less attention than the Majorana fermions near the vortex core. In Refs. 3,28 it has been shown that the edge Majorana fermion localizes at the interface between p-wave superconductor and a topologically trivial insulator if odd number of vortices penetrates superconductor. Edge Majorana modes were studied theoretically[29] in a finite-size heterostructure made of a SC, a ferromagnetic insulator, and semiconductor with strong spin-orbit coupling. It has been argued in Refs. 30,31 that Majorana fermions can arise at the edge of a semi-finite SC placed on the surface of a topological insulator in a magnetic field.

Significant progress with making superconducting islands on the surface of insulators or metals has been achieved in recent years. Observations of vortices and multivortices in the Pb superconducting islands[37–39] and regular structures of the Nb superconducting islands[40] have been reported. These systems are of special interest for possible implementation of the Majorana fermion surface codes for topological quantum computations[41,42].

In our previous works[21,27] we investigated the Majorana fermion in the core of the vortex pinned by a hollow channel in s-wave superconductor placed on the top of topological insulator. This channel removes CdGM levels in the core of the vortex in s-wave superconductor making Majorana fermion robust[21].

In this paper we consider different system: thin cylin-

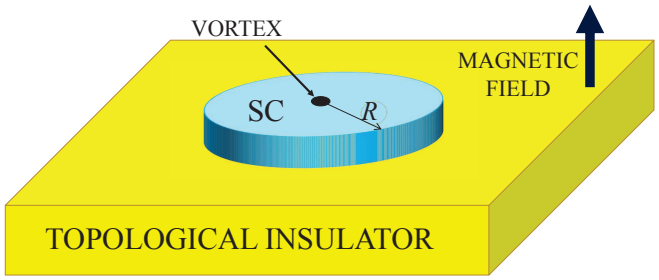

FIG. 1: (Color online) Proposed experimental setup for the detection of edge Majorana fermions. A superconducting (SC) island of radius R (blue) is placed on top of a topological insulator (yellow). An external magnetic field is perpendicular to the interface. The black circle at the center of the superconducting island represents a vortex.

drical s-wave superconducting island of radius R placed on the infinite surface of a topological insulator in a transverse magnetic field B (see Fig. 1). If the island traps a vortex, two Majorana fermions are induced, one at the vortex core in the center of the island and the other at the island edge.

This paper studies the Majorana states localized near the edge of a superconducting island. Edge Majorana states exist only if the vorticity l threading the island is odd, and disappear if l is even or zero. The energy splitting between edge and vortex core Majorana fermions decays exponentially, when increasing the radius of the island. We will demonstrate that the edge Majorana fermion is robust: the gap between the Majorana fermion state and the edge excited state is of the order of the induced superconducting gap. This makes the edge Majorana state promising for experimental observation, and, possibly, manipulation.

The presentation below is organized as follows. In Sec. II we derive the Bogolyubov-de Gennes equations for our system. In Sec. III we investigate modes with zero energy for different number of vortices in the island. In Sec. IV the system with a single vortex is considered. In Sec. V the obtained results are discussed, and conclusions are presented.

II. BOGOLYUBOV-DE GENNES EQUATIONS

A. Microscopic model

Our system is shown in Fig. 1. It consists of a thin cylindrical superconducting island of radius R placed on the surface of a topological insulator. The entire heterostructure is in a magnetic field perpendicular to the topological insulator surface.

To study the microscopic properties of such a system we will use the formalism of Ref. 19. The Hamiltonian can be written as

$$H = H_{\rm TI} + H_{\rm SC} + T + T^\dagger, \tag{1}$$

where $H_{\rm TI}$ describes the topological insulator (TI), $H_{\rm SC}$ describes the s-wave superconductor (SC). The term T accounts for the tunneling from the TI to the SC, while $T^\dagger$ represents the opposite processes: tunneling from the SC to the TI. The corresponding Bogolyubov-de Gennes equations are (after setting $\hbar = e = c = 1$)

$$H_{\rm TI}\psi_{\rm TI} + T^\dagger\psi_{\rm SC} = \omega\psi_{\rm TI}, \tag{2}$$

$$H_{\rm SC}\psi_{\rm SC} + T\psi_{\rm TI} = \omega\psi_{\rm SC}. \tag{3}$$

The terms $H_{\rm TI}$, and $H_{\rm SC}$ can be written as 4×4 matrices in the Nambu basis

$$\begin{aligned} H_{\rm TI} &= [iv(\sigma\cdot\nabla_r) - U(\mathbf{r})]\tau_z + v(\sigma\cdot\mathbf{A})\tau_0, \\ H_{\rm SC} &= -\left[E_{\rm F} + \frac{(\nabla_{\mathbf{R}} - i\mathbf{A}\tau_z)^2}{2m}\right]\tau_z \\ &+ \Delta'(\mathbf{R})\tau_x + \Delta''(\mathbf{R})\tau_y, \end{aligned} \tag{4}$$

and $T = \tau_z\mathcal{T}(\mathbf{R}-\mathbf{r})$. In these equations, $\mathbf{R} = (x, y, z)$ is a point in the bulk of the SC, $\mathbf{r} = (x, y)$ is a point on the surface of the TI, σ_j, τ_j are the spin and charge Pauli matrices, Δ', Δ'' are the real and imaginary parts of the order parameter in the s-wave superconductor, v is the Fermi velocity of the electrons on the surface of the TI, $E_{\rm F}$ is the Fermi energy in the SC, $U(r)$ is a gate voltage applied to control the Fermi level in the TI, and $\mathbf{A}$ is the vector potential of the magnetic field. The wave functions $\psi_{\rm TI,\,SC}$ are four-component spinors

$$\psi_{\rm TI,\,SC} = [u_\uparrow, u_\downarrow, v_\downarrow, -v_\uparrow]^T. \tag{5}$$

It is easy to check that H satisfies the following charge-conjugation symmetry condition

$$\begin{aligned} &\{H, \Xi\} = 0, \\ &\Xi = \sigma_y\tau_y K, \end{aligned} \tag{6}$$

where K is the complex conjugation operator. Consequently, for every eigenstate ψ of the Hamiltonian H with a non-zero eigenenergy $\omega \neq 0$, an eigenstate $\Xi\psi$ with eigenenergy $-\omega$ exists. The latter symmetry is robust: small disorder does not destroy this property.

B. Effective Hamiltonian

In this subsection we will derive the effective description for the wave function of the electrons on the surface of the TI. To this end we exclude $\psi_{\rm SC}$ from Eqs. (2) and (3) to obtain

$$(H_{\rm TI} + \Sigma)\psi_{\rm TI} = \omega\psi_{\rm TI}, \tag{7}$$

$$\Sigma = T^\dagger(\omega - H_{\rm SC})^{-1}T. \tag{8}$$

We are interested in the bound states with energies lying within the superconducting energy gap, $|\omega| < |\Delta|$. In this case, the self-energy matrix Σ was calculated in Refs. 19,

21. For the low-lying electron states with wave vectors $\mathbf{k}$ near the Dirac cone apex $\mathbf{M}$ in the Brillouin zone of the TI, $\mathbf{k} \approx \mathbf{M}$, the self-energy is equal to

$$\Sigma_{\mathbf{M},\omega} = \lambda \frac{\Delta\tau_x - \omega\tau_0}{\sqrt{|\Delta|^2 - \omega^2}} - \delta U \tau_z, \tag{9}$$

where τ_0 is the 2×2 unit matrix. This expression for Σ is independent of $\mathbf{A}$. Such an approximation is valid for weak magnetic fields, which is assumed to be the case everywhere in this paper. The parameter λ has the dimension of energy. It characterizes the transparency of the interface between the TI and the SC: when $\lambda \sim E_{\rm F}$ ($\lambda \ll E_{\rm F}$), the barrier is transparent (non-transparent). The value $\delta U = O(\lambda)$ is the shift of the chemical potential of the TI due to doping by the carriers coming from the SC.

Using Eq. (9) we can rewrite the Bogolyubov-de Gennes equation (7) in the form

$$H_{\rm eff}\psi_{\rm TI} = \omega\psi_{\rm TI}, \tag{10}$$

where the effective Hamiltonian $H_{\rm eff}$ equals to

$$\begin{aligned} H_{\rm eff} &= [i\tilde{v}(\omega)(\sigma\cdot\nabla_{\mathbf{r}}) - \tilde{U}(\omega)]\tau_z + \tilde{v}(\omega)(\sigma\cdot\mathbf{A})\tau_0 \\ &+ \tilde{\Delta}'(\omega)\tau_x + \tilde{\Delta}''(\omega)\tau_y. \end{aligned} \tag{11}$$

The renormalized parameters of the effective Hamiltonian are

$$\tilde{v}(\omega) = \frac{v\sqrt{|\Delta|^2 - \omega^2}}{\sqrt{|\Delta|^2 - \omega^2} + \lambda}, \tag{12}$$

$$\tilde{U}(\omega) = \frac{(U + \delta U)\sqrt{|\Delta|^2 - \omega^2}}{\sqrt{|\Delta|^2 - \omega^2} + \lambda}, \tag{13}$$

$$\tilde{\Delta}(\omega) = \frac{\Delta\lambda}{\sqrt{|\Delta|^2 - \omega^2} + \lambda}. \tag{14}$$

It is also convenient to define the renormalized coherence length:

$$\tilde{\xi}(\omega) = \frac{v\sqrt{|\Delta|^2 - \omega^2}}{\Delta\lambda} = \xi\frac{\sqrt{|\Delta|^2 - \omega^2}}{\lambda}. \tag{15}$$

If the Hamiltonian parameters are independent of $\mathbf{r}$, then the eigenstates of the effective Hamiltonian obey the inequality $|\omega| > \Delta_{\rm TI}$, where the quantity $\Delta_{\rm TI}$ satisfies the following equation:

$$\frac{\Delta_{\rm TI}}{\lambda} = \sqrt{\frac{\Delta - \Delta_{\rm TI}}{\Delta + \Delta_{\rm TI}}}. \tag{16}$$

The physical meaning of $\Delta_{\rm TI}$ is the proximity-induced superconducting gap on the surface of the TI.

C. Equations for the effective wave function

Further, we assume that the island radius R is much larger than the SC coherence length ξ_{SC}.

$$R \gg \xi_{SC} \tag{17}$$

We are looking for solutions of Eq. (10) which correspond to bound states. The energies ω of such eigenstates are smaller than the proximity-induced gap $\Delta_{\rm TI}$, in Eq. (16). If an Abrikosov vortex with vorticity l is trapped in the island, the order parameter $\Delta(\mathbf{r})$ can be expressed as

$$\Delta(\mathbf{r}) = |\Delta(r)| \exp\left(-il\theta\right), \tag{18}$$

where r and θ are the polar coordinates, and $|\Delta(r)| \to |\Delta|$, when $r \gg \xi$. If the island radius R is large, $R \gg \tilde{\xi}$, $|\Delta(r)|$ can be approximated as

$$|\Delta(r)| = |\Delta|\Theta(R - r), \tag{19}$$

where $\Theta(r)$ is the Heaviside step function. In the geometry shown in Fig. 1, the vector potential can be written as $A_z = A_r = 0$, $A_\theta = A(r)$. This choice of the vector potential corresponds to the magnetic field

$$H_z = \frac{1}{r}\frac{d(rA)}{dr}. \tag{20}$$

Let us introduce a spinor F

$$\begin{aligned} \psi_{\rm TI} &= \exp[-i\theta(l\tau_z - \sigma_z)/2 + i\mu\theta]F^\mu(r), \\ F^\mu &= (f_1^\mu, f_2^\mu, f_3^\mu, -f_4^\mu)^T. \end{aligned} \tag{21}$$

Here μ is the total angular momentum of an eigenstate. The transformation Eq. (21) is well-defined only when

$$j = \mu + \frac{l+1}{2} \tag{22}$$

is an integer. In other words, when the number of vortices l is odd (even), the angular momentum μ is an integer (half-integer).

Substituting Eqs. (11), (14), and (21) in Eq. (10) we derive

$$\begin{aligned} i\tilde{v}\left(\frac{d}{dr} + \frac{2\mu + l + 1}{2r} - A(r)\right) f_2^\mu + |\tilde{\Delta}| f_3^\mu - (\omega + \tilde{U}) f_1^\mu = 0, \\ i\tilde{v}\left(\frac{d}{dr} - \frac{2\mu + l - 1}{2r} + A(r)\right) f_1^\mu - |\tilde{\Delta}| f_4^\mu - (\omega + \tilde{U}) f_2^\mu = 0, \\ i\tilde{v}\left(\frac{d}{dr} + \frac{2\mu - l + 1}{2r} + A(r)\right) f_4^\mu + |\tilde{\Delta}| f_1^\mu - (\omega - \tilde{U}) f_3^\mu = 0, \\ i\tilde{v}\left(\frac{d}{dr} - \frac{2\mu - l - 1}{2r} - A(r)\right) f_3^\mu - |\tilde{\Delta}| f_2^\mu - (\omega - \tilde{U}) f_4^\mu = 0. \end{aligned} \tag{23}$$

Equations (23) have the following symmetries: (i) $\mu \leftrightarrow -\mu$, $f_4 \leftrightarrow if_1$, $f_3 \leftrightarrow if_2$, $\tilde{U} \leftrightarrow -\tilde{U}$, and (ii) $A(r) \leftrightarrow -A(r)$, $f_1 \leftrightarrow f_2$, $f_3 \leftrightarrow -f_4$, $l \leftrightarrow -l$, $\mu \leftrightarrow -\mu$. Therefore, we can consider further only $\mu, A(r) \geq 0$.

III. ZERO-ENERGY SOLUTIONS

If $\omega, \tilde{U} = 0$, the system of Eqs. (23) decouples into two sets of equations

$$i\tilde{v}\left(\frac{d}{dr} - \frac{2\mu + l - 1}{2r} + A(r)\right) f_1^\mu - |\tilde{\Delta}| f_4^\mu = 0,$$
$$i\tilde{v}\left(\frac{d}{dr} + \frac{2\mu - l + 1}{2r} + A(r)\right) f_4^\mu + |\tilde{\Delta}| f_1^\mu = 0, \quad (24)$$

and

$$i\tilde{v}\left(\frac{d}{dr} + \frac{2\mu + l + 1}{2r} - A(r)\right) f_2^\mu + |\tilde{\Delta}| f_3^\mu = 0,$$
$$i\tilde{v}\left(\frac{d}{dr} - \frac{2\mu - l - 1}{2r} - A(r)\right) f_3^\mu - |\tilde{\Delta}| f_2^\mu = 0. \quad (25)$$

The parameter $|\tilde{\Delta}|$ is zero outside the SC island area according to Eqs. (19) and (14). It is also zero at the center of the vortex core. In this paper we are mainly interested in the states localized at the edge of the island and the details related to the states in the vortex core are not of importance here. Then, for simplicity, we approximate the vortex core of the vortex with vorticity l by a cylindrical hole with a radius about the coherence length $\tilde{\xi}$.

A. System without vortices

Let us assume first that there are no vortices in the island. The magnetic field localizes a zero mode near the edge of the island. However, we show that this mode is not a robust Majorana fermion.

In the absence of vortices, the SC order parameter Δ is non-zero in the SC island and the solutions of Eqs. (24) and (25) which are regular at $r = 0$ can be expressed in terms of the modified Bessel functions $I_m(x)$

$$f_1 = C_1 \exp\left(-\int_0^r A(r')dr'\right) I_{\mu-1/2}\left(\frac{\lambda r}{v}\right),$$
$$f_4 = -iC_1 \exp\left(-\int_0^r A(r')dr'\right) I_{\mu+1/2}\left(\frac{\lambda r}{v}\right),$$
$$f_2 = C_2 \exp\left(\int_0^r A(r')dr'\right) I_{\mu+1/2}\left(\frac{\lambda r}{v}\right),$$
$$f_3 = iC_2 \exp\left(\int_0^r A(r')dr'\right) I_{\mu-1/2}\left(\frac{\lambda r}{v}\right). \quad (26)$$

Outside the island, where $\tilde{\Delta} = 0$, the solution of Eqs. (24) and (25) becomes

$$f_1 = A_1 \exp\left(-\int_0^r A(r')dr'\right) r^{\mu-\frac{1}{2}},$$
$$f_4 = A_4 \exp\left(-\int_0^r A(r')dr'\right) r^{-\frac{1}{2}-\mu},$$
$$f_2 = A_2 \exp\left(\int_0^r A(r')dr'\right) r^{-\mu-\frac{1}{2}},$$
$$f_3 = A_3 \exp\left(\int_0^r A(r')dr'\right) r^{\mu-\frac{1}{2}}. \quad (27)$$

The functions f_2 and f_3 diverge when $r \to +\infty$; then, $A_2 = A_3 = 0$ or $f_2 = f_3 = 0$. Matching solutions at $r = R$, one completes the derivation of the wave function.

These eigenfunctions correspond to the $\omega = 0$ Landau level, whose states are weakly corrected to account for the presence of the superconducting island. They are not Majorana fermion states, and a weak perturbation of the Hamiltonian may shift their eigenenergies away from zero value.

B. System with vortices

In this subsection we study a system with vortices. Since we are mainly interested in edge states and a relatively small SC island, we assume that the magnetic flux captured in the SC island forms a multivortex with vorticity l and further assume that the SC order parameter in this vortex behaves like a Heaviside step function $\tilde{\Delta}(r) = \tilde{\Delta}\Theta(r - \tilde{\xi})$. This simplification neglects the CdGM states inside the superconductor, and thus, it can significantly affect the Majorana state localized near the vortex core. However, the edge-localized Majorana fermion is fairly insensitive to the details at the center of the island, because its wave function decays quickly away from the edge.

Under these assumptions, the solutions of Eqs. (24) and (25) outside of the island $r > R$, and inside of the vortex core $r < \tilde{\xi}$, can be expressed as

$$f_1 = C_1 \exp\left(-\int_0^r A(r')dr'\right) r^{\mu+\frac{l-1}{2}},$$
$$f_4 = C_4 \exp\left(-\int_0^r A(r')dr'\right) r^{\frac{l-1}{2}-\mu}, \quad (28)$$

and

$$f_2 = C_2 \exp\left(\int_0^r A(r')dr'\right) r^{-\mu-\frac{l+1}{2}},$$
$$f_3 = C_3 \exp\left(\int_0^r A(r')dr'\right) r^{\mu-\frac{l+1}{2}},$$

where C_i are constants (for $r < \tilde{\xi}$ these constants may be different from the constants at $r > R$). The functions f_2 and f_3 diverge when $r \to \infty$, and also f_2 diverges when $r \to 0$. Then, as it follows from Eqs. (25), a regular solution exists only if $f_2 = f_3 = 0$ in the whole space.

Inside the SC island a wave function can be expressed as a sum of two distinctly dissimilar solutions of Eq. (24). A solution of the first type is localized near the vortex core:

$$f_1 = C_2' \exp\left(-\int_0^r A(r')dr'\right) r^{\frac{l}{2}} K_{\mu-1/2}\left(\frac{\lambda r}{v}\right),$$
$$f_4 = iC_2' \exp\left(-\int_0^r A(r')dr'\right) r^{\frac{l}{2}} K_{\mu+1/2}\left(\frac{\lambda r}{v}\right). \quad (29)$$

Here $C_{1,2}'$ are constants, and $K_n(x)$ is the modified Bessel function. Since K_n diverges at $x = 0$, the function f_4 can be normalized only if $\mu < (l+1)/2$. Using the symmetry between positive and negative μ, one can generalize this inequality for arbitrary μ:

$$|\mu| < \frac{l+1}{2}. \quad (30)$$

If μ violates this condition, then Eq. (29) does not define a valid eigenstate.

Unlike Eq. (29), which describes eigenfunctions localized at $r = 0$, a solution of the second type grows toward the edge of the island: for $r < R$ one can write

$$f_1 = C_1' \exp\left(-\int_0^r A(r')dr'\right) r^{\frac{l}{2}} I_{\mu-1/2}\left(\frac{\lambda r}{v}\right),$$
$$f_4 = -iC_1' \exp\left(-\int_0^r A(r')dr'\right) r^{\frac{l}{2}} I_{\mu+1/2}\left(\frac{\lambda r}{v}\right), \quad (31)$$

where I_n is the modified Bessel function of the second kind. Outside the island ($r > R$) the eigenfunction is defined by Eq. (28). Most of the wave function weight is localized away from the island center. The value of r, where the weight is concentrated, grows as $|\mu|$ increases. In the limit $|\mu| \to \infty$, the wave function is virtually unaffected by the presence of a superconducting island at the origin. Thus, for large $|\mu|$ the eigenstates described by Eq. (31) become indistinguishable from the states belonging to the $\omega = 0$ Landau level of the Dirac-Weyl electrons.

Majorana fermion states correspond to $\mu = 0$ solutions. In finite systems these states appear in pairs. In our case, one Majorana fermion is localized near the origin and another is localized at the edge of the island. Inside the island their wave functions are given by Eq. (29) and Eq. (31). Outside the island, Eq. (28) must be used.

To demonstrate the "Majorana nature" of the $\mu = 0$ solutions, let us calculate the first-order corrections to the energies of the states Eq. (31) caused by a non-zero, but small, $\tilde{U}$:

$$\delta\omega_{l\mu} = \tilde{U} C_{l\mu} 2\pi G, \quad (32)$$
$$G = \int_{r>R} dr r^l R e^{-2\int_0^r A(r')dr'} \left(\left[\frac{r}{R}\right]^{2\mu} - \left[\frac{r}{R}\right]^{-2\mu}\right) +$$
$$\int_{r<\xi} dr r^l R e^{-2\int_0^r A(r')dr'} \left(\left[\frac{r}{\xi}\right]^{2\mu} - \left[\frac{r}{\xi}\right]^{-2\mu}\right) +$$
$$\int_{\xi<r<R} dr r^{l+1} e^{-2\int_0^r A(r')dr'} \left(\frac{I^2_{\mu-1/2}\left(\frac{\lambda r}{v}\right)}{I^2_{\mu-1/2}\left(\frac{\lambda R}{v}\right)} - \frac{I^2_{\mu+1/2}\left(\frac{\lambda r}{v}\right)}{I^2_{\mu+1/2}\left(\frac{\lambda R}{v}\right)}\right),$$

where $C_{l\mu}$ are wave function normalization constants. For states localized near the vortex core of the vortex, we have a similar result with the modified Bessel functions $I_{\mu\pm1/2}$ replaced by the modified Bessel functions $K_{\mu\pm1/2}$.

It follows from Eq. (32) that, if $\mu = 0$, the correction vanishes identically. Moreover, one can demonstrate that the $\mu = 0$ states are invariant under the action of the charge-conjugation operator Ξ, Eq. (6). Thus, these eigenstates are topologically-protected mixtures of electron and hole states.

For all other values of μ this correction is nonzero. Thus, the zero-energy states with $\mu \neq 0$ are not topologically-protected from the local perturbations of the chemical potential. In particular, the robustness of the zero-energy modes against variations of the gate voltage may be used to distinguish Majorana states from conventional Dirac fermions.

Finally, we would like to remind that, since μ is an integer only for odd l, see Eq. (22), we must have an odd number of vortices on the island to generate Majorana fermion states.

IV. SINGLE VORTEX

In this section we study a system with a single vortex, $l = 1$, which is the simplest in terms of a possible experimental realization. We start with the case $\tilde{U} = 0$. According to Eqs. (31) the wave function of the zero-energy state with $\mu = 0$ localized near the vortex core

is

$$\psi_v = B_v e^{-i\frac{\pi}{4}} e^{-\int_0^r A(r')dr'} e^{-\int_0^r \frac{\tilde{\Delta}(r')}{\tilde{v}}dr'} \begin{bmatrix} i \\ 0 \\ 0 \\ -1 \end{bmatrix}, \qquad (33)$$

where we used the explicit expression for the modified Bessel function of half-integer order. For the edge zero-energy eigenstate, the wave function is [see Eqs. (29)]

$$\psi_e = B_e e^{-i\frac{\pi}{4}} e^{-\int_0^r A(r')dr'} e^{\int_0^r \frac{\tilde{\Delta}(r')}{\tilde{v}}dr'} \begin{bmatrix} 1 \\ 0 \\ 0 \\ -i \end{bmatrix}. \qquad (34)$$

Here B_v and B_e are normalizing coefficients, which we choose real. Applying the particle-hole-conjugation operator Ξ, we obtain that $\Xi\psi_{v(e)} = \psi_{v(e)}$ by direct calculations. Hence, ψ_v and ψ_e are Majorana fermion wave functions.

A. Zero-mode splitting

The hybridization between the vortex core and the edge Majorana fermions can, in general, split the degenerate zero level. The splitting is zero in the case $\tilde{U} = 0$ (see also Ref. 14). If $\tilde{U} \neq 0$, the degeneracy is lifted, and Majorana fermions at the vortex core and at the edge form the two usual Dirac states. The wave functions of these states can be written as $\psi_\pm = (\psi_v \mp i\psi_e)/2$. These functions satisfy the particle-hole symmetry of the Bogolyubov-de Gennes equations, $\Xi\psi_+ = \psi_-$. If we denote the splitting energy as $2E_+$, then, the wave function ψ_+ corresponds to E_+, while ψ_- corresponds to $-E_+$. Let us assume that $\tilde{U}$ is small. The first-order contribution to the energy splitting becomes

$$E_+ = \tilde{U}\langle\psi_+|\tau_z|\psi_+\rangle. \qquad (35)$$

It is reasonable to assume that the applied magnetic field is smaller than the upper critical field, that is, $l_b \gg \tilde{\xi}$, where l_b is the magnetic length, which satisfies $l_b = B^{-1/2}$, in the units used here. In this case we can neglect the effect of the magnetic field on the wave functions near the vortex core.[25] Further, if the SC island is not large:

$$R \ll l_b, \qquad (36)$$

then, using Eqs. (33), (34) and (35) we derive an estimate for the energy shift E_+ in the form

$$E_+ \propto -\frac{\tilde{U} l_b}{\tilde{\xi}(0)} \exp\left[-R/\tilde{\xi}(0)\right]. \qquad (37)$$

One can now see that Majorana fermion states are robust against chemical potential variations if the radius of the SC island is large, in the sense that

$$R \gg \tilde{\xi}(0) = \frac{v}{\lambda}. \qquad (38)$$

This condition suggests that the growth of the tunneling parameter λ improves the isolation of the two Majorana fermions from each other, which is a desirable property for reliable Majorana state detection.

B. Excited states

Now we calculate the energies of the excited states localized near the SC island edge, assuming that both Eq. (36) and Eq. (38) are valid, and $\tilde{U} = 0$. It is implied for simplicity that the magnetic field penetrates the island uniformly, so, $A(r) = r/2l_b^2$. In this paper, the states localized near the vortex core[21,26,27] are not discussed, because, when the inequality Eq. (38) is valid, the vortex core states do not mix with the edge states, and may be neglected.

When $\omega \neq 0$, $\tilde{U} = 0$, $l = 1$, and $\tilde{\Delta} = 0$, the system Eq. (23) decouples. As a result, for $r > R$ we have two independent systems of equations: one for the electron components $f_{1,2}$, another for the hole component $f_{3,4}$:

$$\begin{aligned} i\tilde{v}\left(\frac{d}{dr} + \frac{\mu+1}{r} - \frac{r}{2l_b^2}\right) f_2^\mu - \omega f_1^\mu &= 0, \\ i\tilde{v}\left(\frac{d}{dr} - \frac{\mu}{r} + \frac{r}{2l_b^2}\right) f_1^\mu - \omega f_2^\mu &= 0, \\ i\tilde{v}\left(\frac{d}{dr} + \frac{\mu}{r} + \frac{r}{2l_b^2}\right) f_4^\mu - \omega f_3^\mu &= 0, \\ i\tilde{v}\left(\frac{d}{dr} - \frac{\mu-1}{r} - \frac{r}{2l_b^2}\right) f_3^\mu - \omega f_4^\mu &= 0. \end{aligned} \qquad (39)$$

Note that after the transformation $f_4^\mu \to i f_1^{-\mu}$ and $f_3^\mu \to i f_2^{-\mu}$, the first two equations and the second two equations exchange places. Thus, we can solve only the equations for $f_{1,2}$. Substituting f_2, one derives for f_1:

$$\frac{d^2 f_1^\mu}{dr^2} + \frac{1}{r}\frac{d f_1^\mu}{dr} + f_1^\mu\left(\frac{\mu+1}{l_b^2} - \frac{\mu^2}{r^2} - \frac{r^2}{4l_b^4} + \frac{\omega^2}{\tilde{v}^2}\right) = 0. \qquad (40)$$

Solutions of the latter equation can be expressed in terms of the Tricomi confluent hypergeometric functions, traditionally denoted[32] as $U(a,b,z)$ (do not confuse it with the shift of the chemical potential $U = U(r)$, which is a function of a single variable). As a result we have

$$\begin{aligned} f_1^\mu &= iAr^\mu \exp\left(-\frac{r^2}{4l_b^2}\right) U\left(-\frac{\omega^2 l_b^2}{2\tilde{v}^2}, \mu+1, \frac{r^2}{2l_b^2}\right), \\ f_2^\mu &= \frac{1}{2}Ar^\mu \exp\left(-\frac{r^2}{4l_b^2}\right) U\left(1 - \frac{\omega^2 l_b^2}{2\tilde{v}^2}, \mu+2, \frac{r^2}{2l_b^2}\right). \end{aligned} \qquad (41)$$

If $r \gg l_b^2\omega/\tilde{v}$, these wave functions decay as follows:

$$f_1^\mu = iC \exp\left(-\frac{r^2}{4l_b^2}\right), \; f_2^\mu = C\,\frac{l_b^2\omega}{r\tilde{v}} \exp\left(-\frac{r^2}{4l_b^2}\right); \qquad (42)$$

consequently, they are normalizable. The second linear-independent solution to Eq. (40) diverges when $r \to \infty$,

thus, it is not included. Near the edge ($r \approx R$) we can approximate the functions in Eq. (41) as

$$f_1^\mu = iCJ_\mu\left(\frac{\omega r}{v}\right), \quad f_2^\mu = CJ_{\mu+1}\left(\frac{\omega r}{v}\right), \tag{43}$$

if the condition $l_b\omega/\tilde{v} \gg 1$ is satisfied. Later, we will show that this condition is similar to the initial assumption $l_b \gg R$. The asymptotic behavior given by Eq. (43) may be guessed from Eq. (40). Indeed, near the island edge, $r \gtrsim R$, the terms $r^2/(4l_b^4)$ and $(\mu+1)/l_b^2$ are much smaller than the remaining two, and may be omitted. After this simplification, equation (40) transforms into the Bessel equation.

In the region $r < R$, we can neglect the effect of the vector potential since $R \ll l_b$. We introduce the following linear combinations[21]

$$\begin{aligned} X_1^\mu &= if_1^\mu + f_4^\mu, \quad X_2^\mu = if_1^\mu - f_4^\mu, \\ Y_1^\mu &= if_2^\mu + f_3^\mu, \quad Y_2^\mu = if_2^\mu - f_3^\mu, \end{aligned} \tag{44}$$

where $X_{1,2}$ obey the differential equations:

$$\frac{d^2X_1^\mu}{dr^2} + \frac{1}{r}\frac{dX_1^\mu}{dr} - \left(\frac{1}{[\zeta(\omega)]^2} + \frac{\tilde{\Delta}}{\tilde{v}r} - \frac{\mu^2}{r^2}\right)X_1^\mu = 0,$$

$$\frac{d^2X_2^\mu}{dr^2} + \frac{1}{r}\frac{dX_2^\mu}{dr} - \left(\frac{1}{[\zeta(\omega)]^2} - \frac{\tilde{\Delta}}{\tilde{v}r} + \frac{\mu^2}{r^2}\right)X_2^\mu = 0, \tag{45}$$

$$\text{where} \quad \zeta(\omega) = \frac{\tilde{v}}{\sqrt{|\tilde{\Delta}|^2 - \omega^2}}, \tag{46}$$

and $Y_{1,2}$ can be found according to the relations:

$$\begin{aligned} Y_1^\mu &= \frac{i\tilde{v}}{\omega}\left(\frac{dX_1^\mu}{dr} - \frac{\tilde{\Delta}}{\tilde{v}}X_1^\mu - \frac{\mu}{r}X_2^\mu\right), \\ Y_2^\mu &= \frac{i\tilde{v}}{\omega}\left(\frac{dX_2^\mu}{dr} + \frac{\tilde{\Delta}}{\tilde{v}}X_2^\mu - \frac{\mu}{r}X_1^\mu\right). \end{aligned} \tag{47}$$

As it follows from Eqs. (23), which are regular at $r = 0$, the solutions for $X_{1,2}$ can be expressed in terms of the Whittaker functions[32]

$$X_{1,2}^\mu = \frac{C_{1,2}}{\sqrt{r}}M_{\alpha_{1,2},\mu}\left(\frac{2r}{\zeta(\omega)}\right). \tag{48}$$

$$\text{where} \quad \alpha_{1,2} = \mp\frac{|\tilde{\Delta}|}{2\sqrt{|\tilde{\Delta}|^2 - \omega^2}}, \tag{49}$$

Matching functions f_i at $r = R$ and using asymptotic Eqs. (43), we obtain a transcendental equation for the eigenenergies ω of the sub-gap excited states:

$$\left(\frac{M'_{\alpha_1,\mu}}{\zeta M_{\alpha_1,\mu}} + \frac{M'_{\alpha_2,\mu}}{\zeta M_{\alpha_2,\mu}} - \frac{\mu+1/2}{R} + \frac{\omega J_{\mu+1}}{\tilde{v}J_\mu}\right) \times \left(\frac{M'_{\alpha_1,\mu}}{\zeta M_{\alpha_1,\mu}} + \frac{M'_{\alpha_2,\mu}}{\zeta M_{\alpha_2,\mu}} + \frac{\mu-1/2}{R} - \frac{\omega J_{\mu-1}}{\tilde{v}J_\mu}\right) = \left(\frac{M'_{\alpha_1,\mu}}{\zeta M_{\alpha_1,\mu}} - \frac{M'_{\alpha_2,\mu}}{\zeta M_{\alpha_2,\mu}} - \frac{\tilde{\Delta}}{\tilde{v}}\right)^2. \tag{50}$$

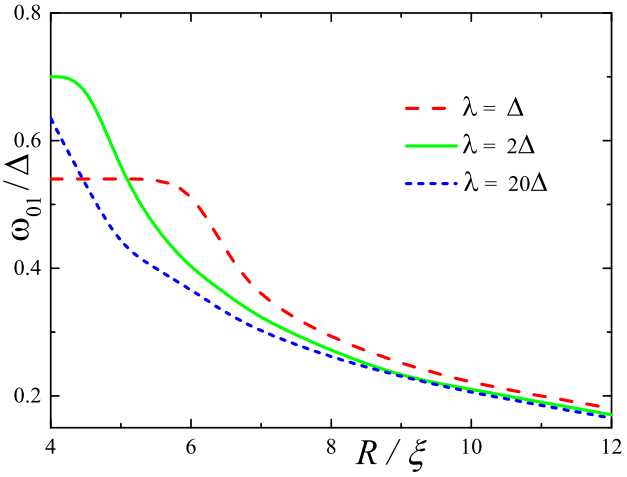

FIG. 2: (Color online) Normalized energy of the first excited state ($\mu = 1$ and $n = 0$) as a function of the normalized island radius R/ξ for different barrier transparencies λ, $BR^2 = R^2/l_b^2 \ll 1$, and according to Eq. (16), $\lambda = 20\Delta$ corresponds to $\Delta_{\rm TI} \approx \Delta$, $\Delta_{\rm TI} \approx 0.75\Delta$, if $\lambda = 2\Delta$; and $\Delta_{\rm TI} \approx 0.54\Delta$, if $\lambda = \Delta$.

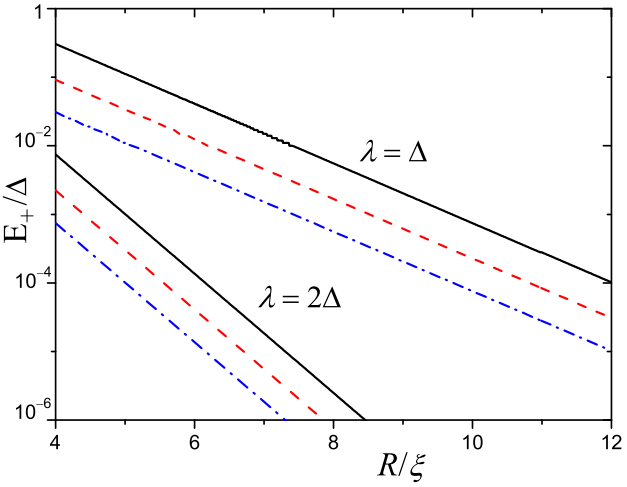

FIG. 3: (Color online) Normalized energy split E_+, Eq. (37), between edge and vortex Majorana fermions as a function of the normalized island radius R/ξ for different barrier transparencies $\lambda = \Delta$ and 2Δ, shift of the Fermi level $U + \delta U = 0.1\Delta$, and different magnetic fields $\sqrt{B}R = R/l_b = 0.003$ (black) solid line, $R/l_b = 0.01$ (red) dashed line, and $R/l_b = 0.03$ (olive) dash-dotted line.

In this expression the Whittaker functions $M_{\alpha,\mu}(z)$ are taken at $z = 2R/\zeta(\omega)$, the Bessel functions $J_\alpha(z)$ at $z = \omega R/v$, and the prime means differentiation over z: $M'_{\alpha,\mu}(z) = dM_{\alpha,\mu}(z)/dz$. An equation similar to Eq. (50) was derived in Ref. 21, and later corrected in Ref. 27.

Each solution of Eq. (50) for the excited states can be characterized by a pair of quantum numbers: orbital number μ and principal number n. A similar classification scheme was used in Refs. 21,25. Our numerical analysis shows that the lowest excited state, localized near the

edge, corresponds to $\mu = 1$ and $n = 0$. The energy of the first excited state ω_{01} as a function of R is plotted in Fig. 2 for different values of the barrier transparencies λ/Δ.

As one can see from this figure, the function $\omega_{01}(R)$ decreases when the island radius R increases. This function has a plateau at low R when the excited state approaches the edge of the continuous spectrum, that is, when ω_{01} is close to $\Delta_{\rm TI}$. The numerical results at large R/ξ and $\lambda \gtrsim \Delta$ can be approximated by the 'particle-in-the-box' formula

$$\omega_{01} \simeq \frac{3\pi}{4}\Delta\left(\frac{\xi}{R}\right) \simeq 2.35\frac{v}{R}. \qquad (51)$$

It follows from the results shown in Fig. 2 that the energy gap between the first excited state and the Majorana fermion is of the order of the energy gap Δ in the SC if $\lambda \gtrsim \Delta$ and $R \leq 10\xi$. Thus, it is not necessary to have an ideal barrier between the TI and SC for a reasonable robustness of the Majorana fermion. For example, if the island radius is $R = 7\xi$ and $\lambda = 2\Delta$, we obtain $\omega_{10} \simeq 0.3\Delta$, which is much larger than the CdGM level spacing $\sim \Delta^2/E_{\rm F}$ for the vortex core states[25] (here E_F is the Fermi level of the SC). The SC island radius $R \sim 5\xi$ is optimal for the stability of the Majorana state if $\lambda \gtrsim \Delta$.

In Fig. 3 we show the dependence of the energy split E_+, Eq. (37), between edge and vortex Majorana fermions as a function of the island radius R/ξ for different barrier transparencies and magnetic fields. Comparison of the results shown in Figs. 2 and 3 demonstrates that the splitting between two Majorana states is small ($E_+ \ll \Delta$) and the Majorana state is rather stable ($\omega_{01} \approx 0.3 - 0.4\Delta$) under realistic values of parameters.

V. DISCUSSION

Below we discuss possible generalizations of our conclusions beyond the constrains assumed in the previous sections, as well as connections of our results to that of other workers.

We study the Majorana fermion near the edge of the s-superconductor island on the top of the topological insulator. In our case, the edge is a boundary between the 2D proximity-induced superconductivity and gapless surface of the topological insulator.

One of the important parameters of the system studied is the island size. The applied magnetic field induces a vortex in the SC island and localizes a Majorana state near the island edge. However, if the island radius is comparable to the length scale $\tilde{\xi}(0) = v/\lambda$ or ξ_{SC}, the stability of the Majorana state deteriorates: first, due to the interaction of the edge and core Majorana fermions and, second, due to tunneling of the CdGM excited states to the edge. Therefore, in a small island there arises a rather peculiar picture of the CdGM states.[33] Thus, the condition (38) is necessary for the existence of well-defined Majorana fermions in the system.

An island of large radius may affect the distribution of the magnetic field in its vicinity. For our calculations we assumed that the magnetic field is uniform. This is true if R is much smaller than the effective London penetration depth $\lambda_{\rm eff}$ in the SC island: $R \ll \lambda_{L\rm eff}$. However, even if this condition is violated, our results survive, provided that the magnetic field is not too strong

$$BR^2 = R^2/l_b^2 \ll 1, \qquad (52)$$

that is, the magnetic flux through the area of the island is smaller than the flux quantum.

The latter inequality is the condition ensuring the validity of our results. The main non-perturbative effect of the magnetic field is the stabilization of a vortex in the island, while the inhomogeneity of the magnetic field in the range $r \ll l_b$ may be studied perturbatively. Indeed, the generation of Majorana states at the vortex core and the edge depends on the parity of the vorticity quantum l, and is completely unaffected by the details of the magnetic field distribution.

Moreover, it can be shown that the relative correction to the energy of the first excited state due to total screening of the magnetic field from the interior of the island is of the order of $R\tilde{\xi}/l_b^2$. To evaluate such a correction $\delta\omega_{01}$, we assume that the magnetic field vanishes for $r < R$. Then, following the procedure presented in the previous section we find

$$\delta\omega_{01} = \frac{\tilde{v}}{2l_b^2}\frac{\int_0^R 2\pi r^2 dr\, \psi^\dagger i\sigma_y\psi}{\int_0^\infty 2\pi r dr\, \psi^\dagger\psi} < \tilde{\Delta}\left(\frac{R\tilde{\xi}}{l_b^2}\right)^2 \sim \omega_{01}\frac{R^2}{l_b^2}\frac{\tilde{\xi}}{R} \ll \omega_{01}, \qquad (53)$$

if the conditions Eq. 52 and $\lambda \gtrsim \Delta$ are valid. For a large island $R \gg \tilde{\xi}$, this correction to the energy is small even if the magnetic field is quite strong $R \sim l_b$.

The case of stronger magnetic field or larger SC island, $R/l_b \gg 1$, requires a separate consideration. However, as before, Majorana fermion may exist only when the island hosts a vortex. This statement is quite natural since the vorticity affects the quantization condition Eq. (22) of μ. As a result, Majorana fermions can exist only if the number of vortices is odd[34]. In addition, for each Majorana fermion, its partner must exist because the fermion parity must be conserved. In the case of a singly-connected SC island the only possibility is to have one Majorana fermion near the island edge and another Majorana fermion near the vortex core, because two Majorana fermions located in the same edge form a Dirac fermion.

In Refs. 30,31 the authors consider a semi-finite SC island on top of a TI in a transverse magnetic field. The Majorana fermion is delocalized at the edge between the SC and the TI. In such a geometry, the condition of single-valuedness of the wave functions Eq. (22) becomes

a momentum quantization rule. If momentum quantization is ignored, then the Majorana fermion can exist at the edge of the SC even in the case of zero vorticity. This is just an unphysical artifact of using an infinite sample.

One of the major driving forces behind the development of Majorana solid state research is the possibility of performing topological quantum computation. To be usable in such a setup, the Majorana fermion must be well separated from non-topological excitations. We demonstrated that the energy of the first excited state localized at the edge could be as large as a fraction of the superconducting gap, see Fig. 2. The time of an elementary braiding operation must be much less than the decoherence time[9] caused by the hybridization of the edge and vortex Majorana fermions. In our system, such decoherence time increases exponentially with the radius of the island, see Eq. (37).

In addition to the excitations pinned at the island edge, there are non-Majorana states localized at $r > R$. These are the Landau levels which we briefly discussed in Sec. III B. Such states with large values of μ are pushed away from the island by the centrifugal force. As a consequence, they cannot affect the Majorana state. At small μ, however, their wave functions can reach the island edge. Fortunately, the Landau levels are separated from each other by a gap of the order of $\Delta_B \sim v/l_B$. Thus, at not-too-weak magnetic fields and finite U these states are shifted from the zero energy by an amount $\sim \Delta_B$.

Scanning tunneling microscopy (STM) might be a useful tool for investigating Majorana fermions[35,36]. In STM experiments, a Majorana fermion could manifest itself as a robust zero-bias peak. A detailed analysis of the STM spectroscopy of the edge Majorana fermions in the presence of vortices is done in Ref. 31. The stability of the zero-bias peak should be checked against variations of the chemical potential or the gate voltage, to distinguish the Majorana fermions from Dirac fermions, as discussed in Section III.

When the magnetic field is varied, the strength of the zero-bias conductance on the island edge should oscillate when the number of vortices changes. These oscillations could be an additional proof of the existence of Majorana fermions. Observations of several vortices and multivortices in superconducting Pb nano-islands were reported.[37,38] Thus, measuring zero-bias peak oscillations as a function of the vorticity is a realizable experimental task. The coordinate dependence of $|\psi|^2$ for the edge and core Majorana states are shown in Fig. 4. The edge Majorana fermion penetrates in the island at the distance $\tilde{\xi}$ and outside the island at the distance l_b. With the decrease of the magnetic field (and the growth of the magnetic length) the peak value in $|\psi|^2$ for the edge Majorana state decreases and if $B \to 0$ the edge Majorana fermion becomes delocalized. Since the density of states is proportional to $|\psi|^2$, such a behavior can be observed as a zero-peak in STM measurement. Note, that the STM measurement could also reveal the zero-peak splitting due to overlapping of the wavefunctions of the edge

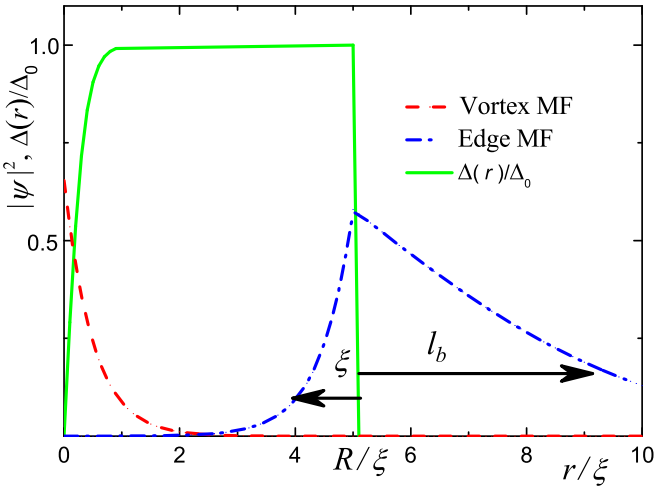

FIG. 4: (Color online) The value $|\psi|^2$, which is proportional to the local density of states, as a function of radial position: (red) dashed line for the vortex Majorana fermion and (blue) dashed-dotted line for the edge Majorana fermion. The local density of states may be measured by the STM. (In the figure the value of $|\psi|^2$ for the edge Majorana fermion is multiplied by 100.) Solid line (green) line shows the proximity-induced superconducting order parameter $\Delta(r)/\Delta_0$, which vanishes when $r > R$, here Δ_0 is the bulk value of Δ and $R = l_b = 5\xi$.

and vortex Majorana fermions in small islands $R \sim \tilde{\xi}$ or due to the close localization of two superconducting islands.

For numerical estimates, let us consider $T_c = 10$ K and $\Delta = 1.76T_c \approx 2$ meV for a BCS-type superconductor. Assuming that $\lambda = 2\Delta \approx 4$ meV, then, $\Delta = \tilde{\Delta}$ and $\xi = 2\tilde{\xi}$. If we take the radius of the island $R = 7\xi$, then, the energy of the first excited state becomes $\omega_{01} \simeq 0.3\Delta \simeq 5$K. To evaluate the possible radius of the SC island we should estimate the value of the coherence length $\xi = v/\Delta$, which depends on the Fermi velocity on the surface of the TI. In Ref. 43 it was reported that $v = 5.0 \times 10^7$ cm/s for the surface of Bi_2Se_3 in vacuum, then, $\xi \approx 200$ nm for the value of the gap chosen here. In Ref. 44 it was obtained that $v = 10^7$ cm/s on the interface between Bi_2Te_3 and a nanoribbon, and then, $\xi \approx 40$ nm. If so, then the appropriate value of R is of the order of several hundred nm. However, it has been reported in Ref. 45 that the Fermi velocity on the surface of Bi_2Te_3 can have a much lower value, $v = 3 \times 10^5$ cm/s, and then, $\xi \approx 1.2$ nm and R could be of the order of several nm, which might be of the order of or lower than the coherence length ξ_{SC} in the bulk of the SC island. The case $R \lesssim \xi_{SC}$ is not optimal for the stability of the edge Majorana fermion because CdGM states in the vortex core in the bulk of the SC can affect the edge states.

To conclude, we studied the electronic properties of a superconducting island in a magnetic field placed on the surface of a topological insulator. Majorana states arise only if a vortex with odd vorticity exists in the superconducting island. Non-topological excitations in our

structure are separated from the Majorana fermion by a significant gap, provided that the parameters are suitably chosen. A Majorana state may be detected in an STM experiment as a zero-bias peak, which is stable against variations of the gate voltage. The zero-bias conductance should oscillate as a function of the magnetic field. We here estimate the optimal parameters for the experimental study of Majorana fermions in our system.

Acknowledgements

We acknowledge partial support by the Dynasty Foundation and ICFPM (MMK), the Ministry of Education and Science of the Russian Federation Grant No. 14Y26.31.0007, RFBR Grant No. 15-02-02128. FN is partially supported by the RIKEN iTHES Project, MURI Center for Dynamic Magneto-Optics via the AFOSR award number FA9550-14-1-0040, and a Grant-in-Aid for Scientific Research (S).

[1] F. Wilczek, *Majorana returns*, Nat. Phys. **5**, 614 (2009).
[2] F. Wilczek, *Majorana modes materialize*, Nature **486**, 195 (2012).
[3] J. Alicea, *New directions in the pursuit of Majorana fermions in solid state systems*, Rep. Prog. Phys. **75**, 076501 (2012).
[4] M. Leijnse and K. Flensberg, *Introduction to topological superconductivity and Majorana fermions*, Semiconductor Science and Technology **27**, 124003 (2012).
[5] C. Beenakker, *Search for Majorana Fermions in Superconductors*, Annual Review of Condensed Matter Physics **4**, 113-136 (2013).
[6] M. Franz, *From particles to nanowires*, Nat. Nanotechnology **8**, 149-152 (2013).
[7] T. D. Stanescu and S. Tewari, *Majorana fermions in semiconductor nanowires*, Journal of Physics: Condensed Matter **25**, 233201 (2013).
[8] S. R. Elliot, M. Franz, *Colloquium: Majorana Fermions in nuclear, particle and solid-state physics*, Rev. Mod. Phys. **87**, 137 (2015).
[9] C. Nayak, S. H. Simon, A. Stern, M. Freedman, S. Das Sarma, *Non-Abelian anyons and topological quantum computation*, Rev. Mod. Phys. **80**, 1083 (2008).
[10] A. Yu. Kitaev, *Fault-tolerant quantum computation by anyons*, Ann. Phys. (NY) 303, 2 (2003).
[11] J. D. Sau, D. J. Clarke, and S. Tewari, *Controlling non-Abelian statistics of Majorana fermions in semiconductor nanowires*, Phys. Rev. B 84, 094505 (2011).
[12] M. Burrello, B. van Heck, A. R. Akhmerov, *Braiding of non-Abelian anyons using pairwise interactions*, Phys. Rev. A **87**, 022343 (2013).
[13] B. van Heck, A. R. Akhmerov, F. Hassler, M. Burrello, C. W. J. Beenakker, *Coulomb-assisted braiding of Majorana fermions in a Josephson junction array*, New J. Phys. **14**, 035019 (2012).
[14] M. Cheng, R.M. Lutchyn, V. Galitski, and S. Das Sarma, *Tunneling of anyonic Majorana excitations in topological superconductors*, Phys. Rev. B **82**, 094504 (2010).
[15] V. Mourik, K. Zuo, S. M. Frolov, S. R. Plissard, E. P. A. M. Bakkers, and L. P. Kouwenhoven, *Signatures of Majorana fermions in hybrid superconductor-semiconductor nanowire devices*, Science **336**, 1003 (2012); M. T. Deng, C. L. Yu, G. Y. Huang, M. Larsson, P. Caroff, and H. Q. Xu, *Anomalous Zero-Bias Conductance Peak in a* Nb-In Sb *Nanowire*-Nb *Hybrid Device*, Nano Lett. **12**, 6414 (2012); L. P. Rokhinson, X. Liu, and J. K. Furdyna, *The fractional a.c. Josephson effect in a semiconductor-superconductor nanowire as a signature of Majorana particles*, Nat. Phys. **8**, 795 (2012); A. Das, Y. Ronen, Y. Most, Y. Oreg, M. Heiblum, and H. Shtrikman, *Zero-bias peaks and splitting in an* AlInAs *nanowire topological superconductor as a signature of Majorana fermions*, ibid. **8**, 887 (2012).
[16] E. J. H. Lee, X. Jiang, R. Aguado, G. Katsaros, C. M. Lieber, and S. De Franceschi, *Zero-Bias Anomaly in a Nanowire Quantum Dot Coupled to Superconductors*, Phys. Rev. Lett. **109**, 186802 (2012); A. D. K. Finck, D. J. Van Harlingen, P. K. Mohseni, K. Jung, and X. Li, *Anomalous Modulation of a Zero-Bias Peak in a Hybrid Nanowire-Superconductor Device*, ibid. **110**, 126406 (2013); H. O. H. Churchill, V. Fatemi, K. Grove-Rasmussen, M. T. Deng, P. Caroff, H. Q. Xu, and C. M. Marcus, *Superconductor-nanowire devices from tunneling to the multichannel regime: Zero-bias oscillations and magnetoconductance crossover*, Phys. Rev. B **87**, 241401(R) (2013); E. J. H. Lee, X. Jiang, M. Houzet, R. Aguado, C. M. Lieber, and S. De Franceschi, *Spin-resolved Andreev levels and parity crossings in hybrid superconductorsemiconductor nanostructures*, Nat. Nanotechnol. **9**, 79 (2014).
[17] S. Nadj-Perge, I. K. Drozdov, J. Li, H. Chen, S. Jeon, J. Seo, A. H. MacDonald, B. A. Bernevig, A. Yazdani, *Observation of Majorana fermions in ferromagnetic atomic chains on a superconductor*, Science **346**, 602 (2014).
[18] L. Fu and C.L. Kane, *Superconducting Proximity Effect and Majorana Fermions at the Surface of a Topological Insulator*, Phys. Rev. Lett. **100**, 096407 (2008).
[19] J.D. Sau, R.M. Lutchyn, S. Tewari, and S. Das Sarma, *Robustness of Majorana fermions in proximity-induced superconductors*, Phys. Rev. B **82**, 094522 (2010).
[20] P.A. Ioselevich, M.V. Feigel'man, *Anomalous Josephson current via Majorana bound states in topological insulators*, Phys. Rev. Lett. **106**, 077003 (2011).
[21] A.L. Rakhmanov, A.V. Rozhkov, F. Nori, *Majorana fermions in pinned vortices*, Phys. Rev. B **84**, 075141 (2011).
[22] P.A. Ioselevich, P.M. Ostrovsky, M.V. Feigel'man, *Majorana state on the surface of a disordered three-dimensional*

topological insulator, Phys. Rev. B **86**, 035441 (2012).
[23] M. Snelder, A.A. Golubov, Y. Asano, and A. Brinkman, Phys. Rev. B **85**, 180509(R) (2012).
[24] N. Read and D. Green, *Paired states of fermions in two dimensions with breaking of parity and time-reversal symmetries and the fractional quantum Hall effect*, Phys. Rev. B **61**, 10267 (2000).
[25] C. Caroli, P.G. de Gennes, and J. Matricon, *Bound Fermion states on a vortex line in a type II superconductor*, Phys. Lett. **9**, 307 (1964); R.G. Mints and A.L. Rakhmanov, *On the Energy Spectrum of Excitations in Type-II Superconductors*, Solid State Commun. **16**, 747 (1975).
[26] G. E. Volovik, *Fermion zero modes on vortices in chiral superconductors*, JETP Lett. **70**, 609-614 (1999).
[27] R.S. Akzyanov, A.V. Rozhkov, A.L. Rakhmanov, F. Nori, *Tunneling spectrum of a pinned vortex with a robust Majorana state*, Phys. Rev. B **89**, 085409 (2014).
[28] M. Stone, R. Roy, *Edge modes, edge currents, and gauge invariance in p_x+ip_y superfluids and superconductors*, Phys. Rev. B **69**, 184511 (2004).
[29] Q.-F. Liang, Z. Wang, X. Hu, *Manipulation of Majorana fermions by point-like gate voltage in the Vortex state of a topological superconductor*, EPL **99**, 5 (2012).
[30] R. P. Tiwari, U. Zülicke, and C. Bruder, *Majorana Fermions from Landau Quantization in a Superconductor and Topological-Insulator Hybrid Structure*, Phys. Rev. Lett. **110**, 186805 (2013).
[31] R. P. Tiwari, U. Zülicke, and C. Bruder, *Signatures of tunable Majorana-fermion edge states*, New J. Phys **16**, 025004 (2014).
[32] M. Abramowitz and I.A. Stegun, *Handbook of Mathematical Functions* (NBS, 1972).
[33] N. B. Kopnin, A. S. Mel'nikov, V. I. Pozdnyakova, D. A. Ryzov, I. A. Shereshevskii, V. M. Vinokur, *Giant Oscillations of Energy Levels in Mesoscopic Superconductors*, Phys. Rev. Lett. **95**, 197002 (2005).
[34] S. Tewari, S. Das Sarma, D.-H. Lee, *Index Theorem for the Zero Modes of Majorana Fermion Vortices in Chiral p-Wave Superconductors*, Phys. Rev. Lett. **99**, 037001 (2007).
[35] K. Flensberg, *Tunneling characteristics of a chain of Majorana bound states*, Phys. Rev. B **82**, 180516(R) (2010).
[36] P. A. Ioselevich, and M.V. Feigel'man, *Tunneling conductance due to a discrete spectrum of Andreev states*, New J. Phys. **15**, 055011 (2013).
[37] T. Cren, L. Serrier-Garcia, F. Debontridder, and D. Roditchev, *Vortex Fusion and Giant Vortex States in Confined Superconducting Condensates*, Phys. Rev. Lett. **107**, 097202 (2011).
[38] T. Tominaga, T. Sakamoto, H. Kim, T. Nishio, T. Eguichi, Y. Nasegawa, *Trapping and squeezing of vortices in voids directly observed by scanning tunneling microscopy and spectroscopy*, Phys. Rev. B **87**, 195434 (2013).
[39] D. Roditchev, C. Brun, L. Serrier-Garcia, J. C. Cuevas, V. H. L. Bessa, M. V. Milosevic, F. Debontridder, V. Stolyarov, T.Cren, *Direct observation of Josephson vortex cores*, Nat. Phys. **11**, 332 (2015).
[40] S. Eley, S. Gopalakrishnan, P. M. Goldbart, N. Mason, *Approaching zero-temperature metallic states in mesoscopic superconductornormalsuperconductor arrays*, Nat. Phys. **8**, 59 (2012).
[41] S. Bravyi, B. M. Terhal, B. Leemhuis, *Majorana fermion codes*, New J. Phys. **12**, 083039 (2010).
[42] S. Vijay, T. H. Hsieh, L. Fu, *Majorana Fermion Surface Code for Universal Quantum Computation*, arXiv:1504.01724
[43] H. Zhang, C.-X. Liu, X.-L. Qi, X. Dai, Zh. Fang and S.-C. Zhang, *Topological insulators in* Bi_2Se_3, Bi_2Te_3 *and* Sb_2Te_3 *with a single Dirac cone on the surface*, Nat. Phys. **5**, 438 (2009).
[44] M. Veldhorst, M. Snelder, M. Hoek, T. Gang, V. K. Guduru, X. L. Wang, U. Zeitler, W. G. van der Wiel, A. A. Golubov, H. Hilgenkamp, A. Brinkman, *Josephson supercurrent through a topological insulator surface state*, Nat. Mat. **11**, 417-421 (2012).
[45] A. Wolos, S. Szyszko, A. Dzabinska, M. Kaminska, S.G. Strelecka, A. Hruban, A. Materna, M. Piersa, *Landau-Level Spectroscopy of Relativistic Fermions with Low Fermi Velocity in the* Bi_2Te_3 *Three-Dimensional Topological Insulator*, Phys. Rev. Lett. **109**, 247604 (2012).